Proceeding 20th SEAGC - 3rd AGSSEA Conference in conjunction with 22nd Annual Indonesian National Conference on Geotechnical Engineering. Jakarta - INDONESIA, 6 -7 November 2018. ISBN No. 978-602-17221-6-9

# Plane Strain Ratio and Waling Size Evaluation of Deep Excavation of Kuala Lumpur Using 3D Finite Element Analysis

Jen Shen Ang[1]*, Bin Chen Benson Hsiung[1], Ching Hung[2], A. J. Li[3], J. W. Chen[2]

[1] *Department of Civil Engineering, National Kaohsiung University of Science and Technology, Kaohsiung, Taiwan*
[2]*Department of Civil Engineering, National Cheng- Kung University, Tainan, Taiwan*
[3]*Department of Construction Engineering, National Taiwan University of Science and Technology, Taipei, Taiwan*
*E-mail*: 1102102171@gm.kuas.edu.tw

**ABSTRACT:** This paper presents a study based on 3D Finite Element Analysis of deep excavations in Kuala Lumpur, Malaysia. The ground in Kuala Lumpur mainly consists of a layer of highly permeable sand, occasionally with some thin layers of clay above rock which includes interbedded sandstone, siltstone, shale and mudstone for so called "Kenny Hill Formation" or limestone with sinkholes for so called "KL limestone formation". A common feature is the depth of rock varies in a widely range which leads to challenges of design and construction of excavations. By using 3D finite element analysis together with observational data, it aims to explore plane strain ratio (PSR) of deep excavation of Kuala Lumpur which can indicate impacts from the corner effect associated with distance to the corner. Influences on PSR from certain factors, such as centre- to- centre distance of struts and hard soil stratum/rock depth are also covered and examined in this study. Moreover, individual secant bored piles (SBP) wall have to be adopted for retaining structure of deep excavation in Kuala Lumpur as hydraulic- grab type diaphragm wall can't be constructed in very hard rock, such as limestone and thus steel waling has to be installed in order to connect each SBP, not only providing the function of strut- wall connection. It is not possible to apply 2D analysis to examine waling size in the aspect of function of SBP connection so 3D analysis has to be conducted instead for said purpose. The evaluation of waling size is thus included in this study.
**Keywords:** Deep excavation, Kuala Lumpur, 3D finite element analysis, Plain Strain Ratio, SBP wall, walling size

## 1. INTRODUCTION

Kuala Lumpur is the capital city of Malaysia. Due to the fast development urban area and limited urban public transport service in Kuala Lumpur, additional underground space is required for both private and public uses in the city. The behaviour of walls induces by deep excavation had been studied but limited studies have been reported for excavations in Kuala Lumpur, Malaysia, especially in the aspects of PSR (Plain strain ratio) and evaluation of waling details where deeper basements for the use of both public and private sectors in the future. Furthermore, available and reliable soil data is limited and few of the large-scale deep excavations in the city have been well documented. These are all obstacles to increase the difficulty of studying deep excavation in Kuala Lumpur area.

3D wall behaviour has been studied by using 3D (three-dimensional) FE (Finite element) analysis. The concept of plane strain ratio (PSR) was first proposed by Ou et al. (2006) and it is the ratio of the maximum wall deflection at a section of a wall where distance (d) from the corner to the maximum wall deflection at the section under plane strain conditions. The PSR was adopted in this study to validate the 3D wall behaviour of an excavation in drained material in KLCC (Kuala Lumpur City Centre) area.

One of the most commonly used additional supporting systems in conjunction with retaining walls for deep basement excavation is the steel strut- waler system (Chiew & Leow, 2006). The struts usually consist of an H-section with walers laid across the walls to ensure continuity. On the other hand, for strut-waler connection, the webs of the strut and waler are in two different planes perpendicular to each other. Strut-waler system was adopted in Kuala Lumpur due to the construction of SBP wall. Since the primary bored pile has no reinforcement so it can't take much bending moment, it has to rely on the waler to take bending moment and get better connection.

This paper presents two cases of deep excavation in Kuala Lumpur. One of these two cases is named Case KLCC and the ground is Kenny Hill Formation. The other case is located at Bukit Bintang where the ground is Kuala Lumpur limestone formation which named as Case Waler.

## 2. THE SITES AND PROJECTS BACKGROUND

The case history of excavation in Kenny Hill Formation (Case KLCC) which provided by Law et al. (2016). It is a three- level deep basement, the geometry of basement excavation is rectangular, the width and length of the basement excavation are approximately 43 m x 78 m in plain view (Figure 1). The maximum depth of excavation is 13.2m. 20m deep of diaphragm wall is supported by one level of H-section steel struts. There are ten inclinometers in the site and the location are as figure 1. Kenny Hill formation is residual soils which derived from weathered sedimentary rocks and commonly found in major part of Kuala Lumpur city centre (KLCC) area. The sequence of Kenny Hill Formation along the alignment comprises of interbedded to be the Upper Palaeozoic age. This formation has undergone mild and regional metamorphic materials, such as siltstone and shales/mudstone overlain by stiff over-consolidated soils predominately of sandstone/siltstone to quartzite and schist/phyllite respectively. The ground condition in this study consisted of upper recent alluvium deposits about 8m depth which underlain by residual soils and weathered rocks of Kenny Hill formation. The ground condition at the site consists of a 7.5 m thick of silty sand layer underlain by residual soils of Kenny Hill formation. Upper recent alluvium layer is low SPT- N values Skeptom (1986), mainly consists of loose silty sand material. At the deeper soil layer, the SPT- N value ranges from 15 to 200 blows/300mm and increase with depth (Figure 2). The excavation was completely embedded in drained material. The observation shows that the groundwater table at approximately 2.5m below ground surface.

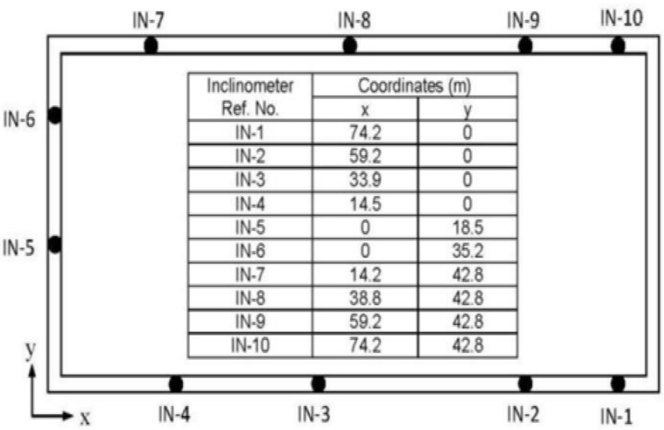


| Inclinometer Ref. No. | Coordinates (m) x | y |
|---|---|---|
| IN-1 | 74.2 | 0 |
| IN-2 | 59.2 | 0 |
| IN-3 | 33.9 | 0 |
| IN-4 | 14.5 | 0 |
| IN-5 | 0 | 18.5 |
| IN-6 | 0 | 35.2 |
| IN-7 | 14.2 | 42.8 |
| IN-8 | 38.8 | 42.8 |
| IN-9 | 59.2 | 42.8 |
| IN-10 | 74.2 | 42.8 |

Figure 1 Plan view of excavation shape and inclinometers arrangement of case KLCC (Law et al. 2016)

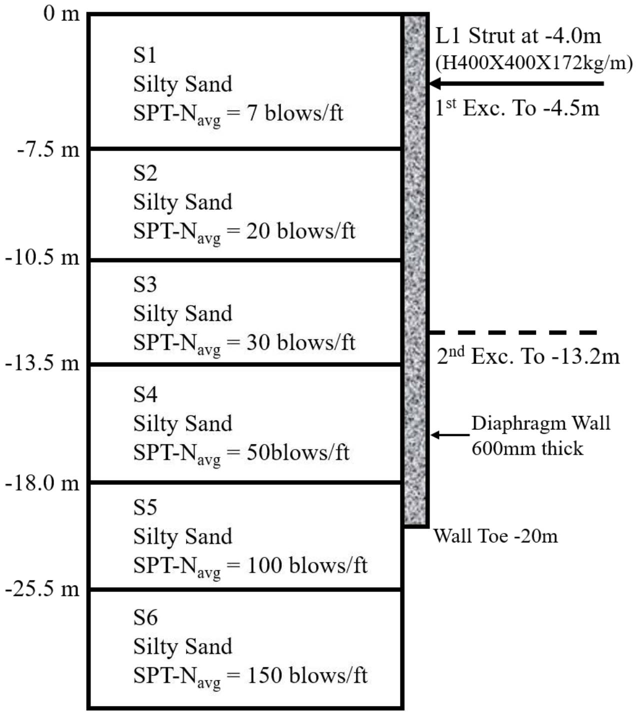


Figure 2 Excavation stages and soil profile in cross-section (Law et al. 2016)

Case Waler is located at Bukit Bintang, the ground of this case is Kuala Lumpur Limestone formation as described previously. Kuala Lumpur Limestone Formation is composed of fine to coarse, white to grey, predominantly recrystallized limestone and dolomites with irregular level of rock below the alluvium and containing numerous voids and solution channels. These features are consistent with classification of Karst terrain according to Waltham & Fokes (2003). Karst topography in limestone is formed by chemical dissolution process when groundwater circulates through the limestone (figure 3), carbon dioxide from the atmosphere is fixed or converted into the soil in aqueous state and combined with rainwater to form carbonic acid, which can dissolve carbonate rocks. Simplified subsurface profile of Kuala Lumpur Limestone formation. Case Waler is one of the underground metro stations in Kuala Lumpur and has to be excavated in Kuala Lumpur limestone formation together with soil above. The maximum excavation depth of Case Waler is 31.5m. There are 4 combination zones of the site, the description of the zones as below are in plan view:

1. Zone 1: Trapezoidal shape with width of 23 m and the zone is connecting with zone 4 and zone 2, the station end is to enable TBM launching.
2. Zone 2: Rectangular shape with width of 23 m and the zone is connecting between zone 1 and zone 3.
3. Zone 3: This zone is complex geometry and it connect with zone 2. TBM launching will at the station ends with 23 m width and the entrance will locate beside the station end.
4. Zone 4: This zone is one of the entrances of the underground station with rectangular shape

Figure 4 shows the geometry of the case Waler excavation. The pit was retained by SBP wall with the strut-waler supporting system, including H-type steel props, ground anchors, H-type steel walers, rock bolts. Curtain and base grouting were carried out to prevent water ingress through rock fissures of sinkholes surrounding the excavation area due to drawdown of groundwater. The embedded depth of retaining wall of Case Waler is shallower than excavation depth since the limestone was considered to be a very stiff material, can be stable without any support system once the excavation reaches the depth of rock. In this case, four TBM (Tunnel boring machine) need to launch from this site, that is the reason there is one section having a very large spacing of strut, which is 17m in order to fit the whole TBM into the pit.

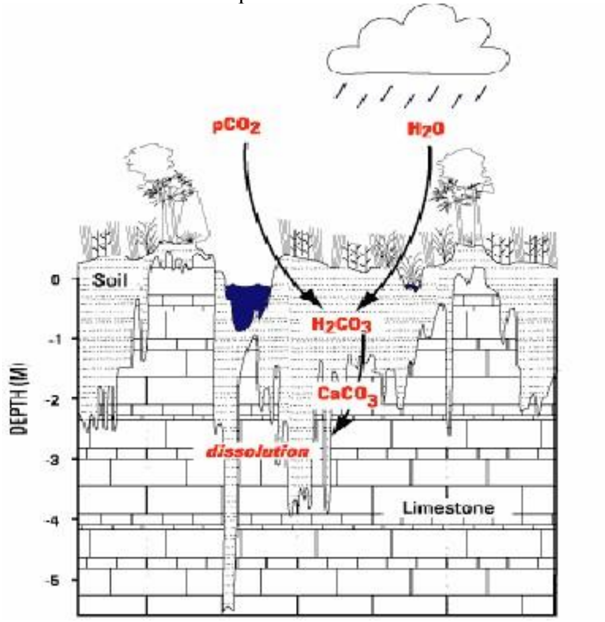


Figure 3 Development of karsts from i-geology

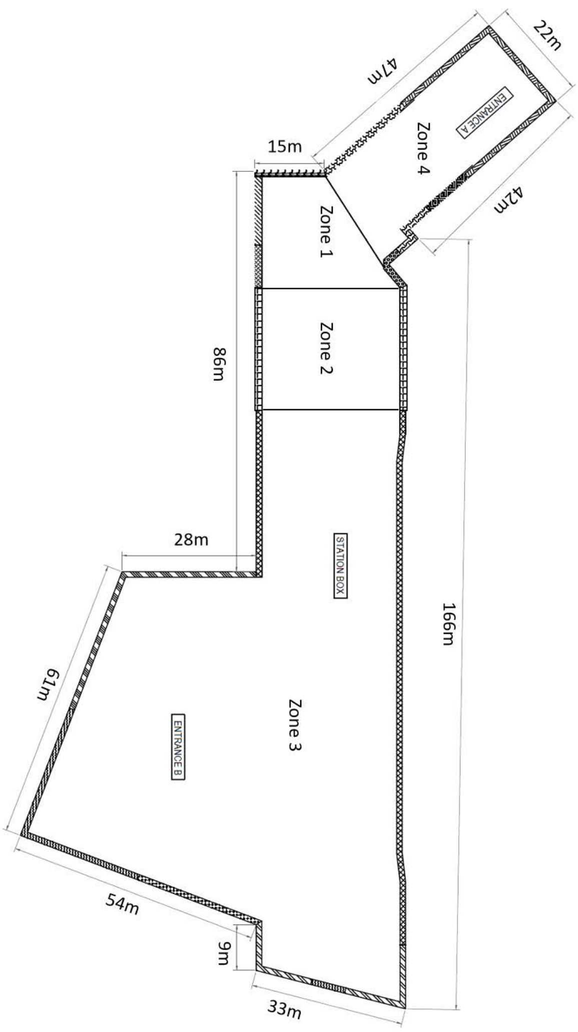


Figure 4 Geometry of case waler

## 3. FINITE ELEMENT ANALYSIS METHOD

### 3.1 Mesh Boundary of Numerical Modeling

The numerical modelling of Case KLCC is built associated with the information which provided by Law et al. (2016), such as mesh boundary and geometry of deep excavation side. The groundwater table is observed at approximately 2.5 m below the ground surface and set the groundwater table into PLAXIS 3D. The mesh boundary and phreatic level are shown as Figure 5. The total nodes in the 3D model are 147,229 and 99,446 is the number of total ten-node tetrahedral elements. The "normal" mesh is applied to the whole model.

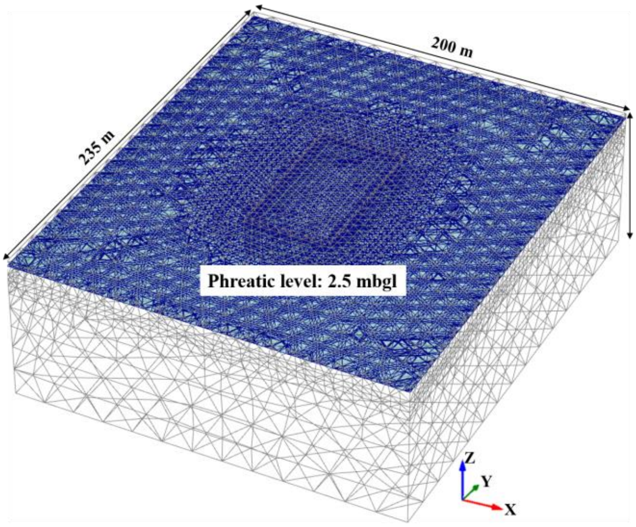


Figure 5 Mesh boundary and phreatic level in PLAXIS 3D

Although the Law et al. (2016) has shown the arrangement of lateral supporting system (strutting system) in horizontal and diagonal, the exactly coordinate and spacing are not given. Therefore, the strutting system is thus assumed to have a horizontal spacing of 6 m in primary wall and 2 m spacing in complementary wall with perpendicular based on local engineering practice in Malaysia and only one-layer strutting system in used Details of strutting system in the model are illustrated in Figure 6.

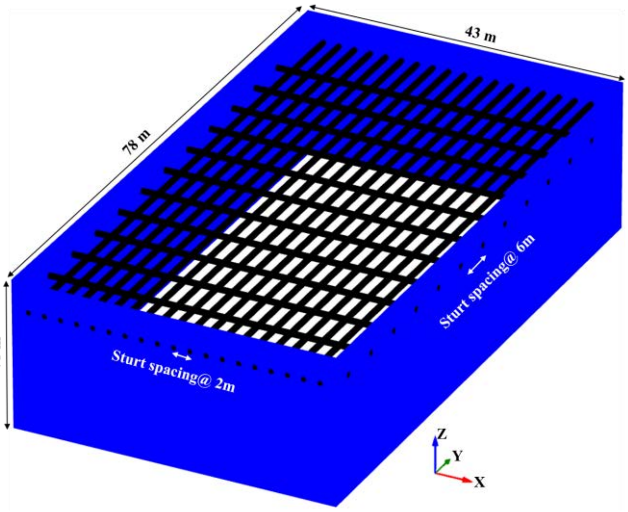


Figure 6 Dimension of retaining wall and struts spacing

For Case Waler, since it aims to evaluate whether the capacity of waler is enough to take the stresses from retaining wall or not so the geometry of whole excavation is not simulated by using PLAXIS 3D in order to shorten time of generation of model and running time of computer operation. A rectangular shape of 3D model is conducted to undertake the analysis. The mesh boundary of PLAXIS 3D is length of 290 m (x), width of 200 m (y), depth of 104.5 m (z) presented as Figure 7. The geometry of excavation is length of 120 m and 30 m for width in plan view and the strut spacing of 6 m with an area of 17 m strut spacing (Figure 8). The purpose excavation level is 31 mbgl and the toe of wall is located at 28 mbgl. The mesh of this model is used "normal" mesh setting. The model consists of 416,761 nodes and 284,581 ten-node tetrahedral elements.

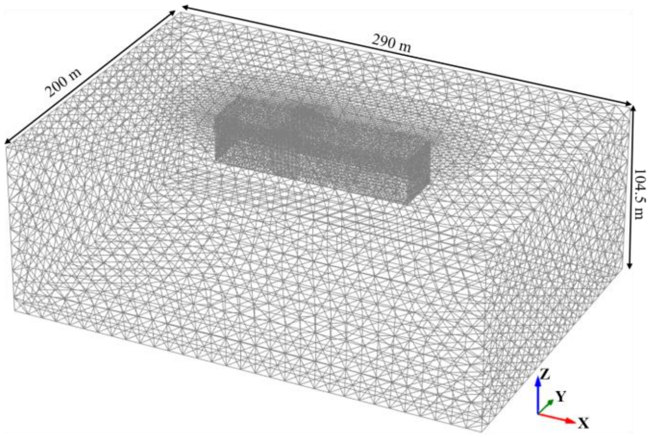


Figure 7 Mesh boundary of PLAXIS 3D in Case waler

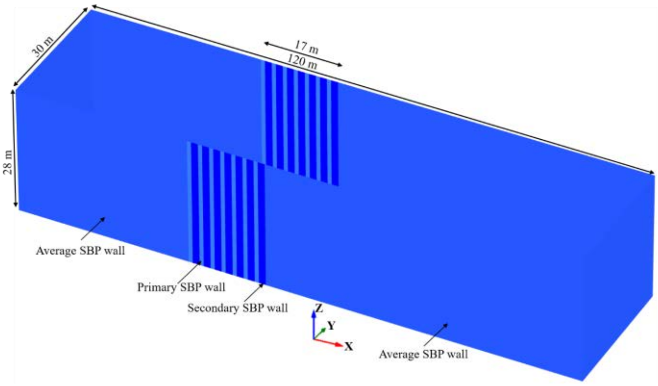


(a)

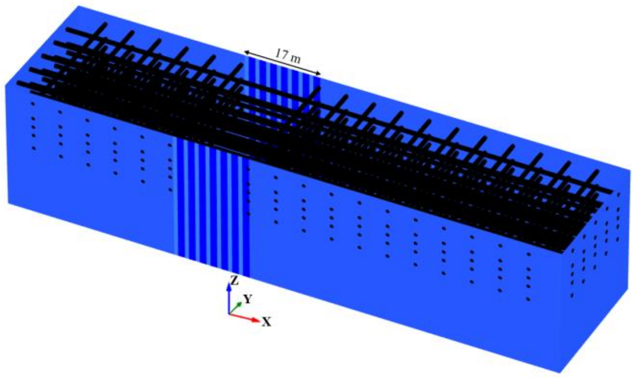


(b)

Figure 8 Detail supporting system in PLAXIS 3D: (a) Plate element (retaining wall); (b) Node to node element (struts)

Based on the interpreted subsoil parameters, the groundwater table is approximately at 1 mbgl and set it in PLAXIS 3D for simulation.

## 3.2 INPUT PARAMETERS

Hardening soil (HS) model is adopted to simulate the soil behaviors in Case KLCC. HS model is an advantage model for simulating the behavior of different types of soil, both soft soils and stiff soils reported by Schanz (1999). Law et al. (2014) highlighted that the general problem in the analysis and design of deep excavations in loose to medium dense sand with shallow meta-sedimentary hard layer which soil tests information is limited and low-quality sampling. Normally, the shear strength of soil can be obtained from laboratory triaxial tests and direct shear tests but not on the stiffness of soil. Due to the reasons, one of the field tests which called Standard Penetration Test (SPT) is conducted to obtain the information of subsoil for geotechnical design and analysis purpose. However, the empirical correlation between stiffness of soil and number of SPT (SPT-N) are used for prediction the ground movement induced by excavation.

The constitutive soil model of HS model used for case history is studied by Law et al. (2016), the performance between numerical analysis and field observation reading are similarly, the empirical correlation is suitable for simulating in the formation. Triaxial secant modulus $E_{50}^{ref}$ with SPT-N is taken as below:

$$E_{50}^{ref} = 2000N \quad (1)$$

The ratios between $E_{50}^{ref}$, $E_{oed}^{ref}$ and $E_{ur}^{ref}$ are as follows:

$$E_{50}^{ref} = E_{oed}^{ref} \quad (2)$$

$$E_{50}^{ref} = E_{ur}^{ref} \quad (3)$$

The simple assumption as suggested by Schanz et al. (1999) and Brinkgreve et al. (2012), the effective stress strength (c' and ϕ') and stiffness parameters adopted in the 2D numerical study are summarized in Table 1. Based on Tan (2010), the ground properties of excavation in residual soils is fully drained condition. Therefore, effective stress analysis (drained material) is performed in the 3D numerical back analysis.

Table 1 Input soil parameters of case KLCC

| **Symbol** | **Unit** | **S1** | **S2** | **S3** | **S4** | **S5** | **S6** |
|---|---|---|---|---|---|---|---|
| c' | kPa | 1 | 5 | 5 | 8 | 15 | 50 |
| ϕ' | ° | 28 | 30 | 31 | 33 | 35 | 35 |
| $E_{50}^{ref}$ | MPa | 15 | 30 | 45 | 75 | 150 | 225 |
| $E_{oed}^{ref}$ | MPa | 15 | 30 | 45 | 75 | 150 | 225 |
| $E_{ur}^{ref}$ | MPa | 45 | 90 | 135 | 225 | 450 | 675 |
| m | - | 0.5 | 0.5 | 0.5 | 0.5 | 0.5 | 0.5 |
| $v_{ur}$ | - | 0.2 | 0.2 | 0.2 | 0.2 | 0.2 | 0.2 |
| $p^{ref}$ | kPa | 100 | 100 | 100 | 100 | 100 | 100 |
| $R_{inter}$ | - | 0.67 | 0.67 | 0.67 | 0.67 | 0.67 | 0.67 |

Linear elastic plate element is used to simulate the diaphragm with 6-node. The Young's modulus of plate element is assumed 19.6 GPa which 70% of the concrete compression stiffness of 28GPa. Assuming the diaphragm wall is "wished-in-place", which means this work does not consider the stress and ground movement during the construction diaphragm such as trench excavation and concreting. Table 2 is the input parameters of plate element (diaphragm wall). A required input parameter is unit weight, due to the overlapping of unit weight and volume between soil element and plate element, so need to subtract the surrounding unit weight of soil for the unit weight of plate element (diaphragm wall). The node to node anchor is used for simulating the steel struts to support diaphragm wall. The input parameter of anchor is EA, where E is the Young's modulus of steel struts, and A is the cross-sectional area of steel struts. 60% of Young's modulus of steel is adopted for the input parameters. The parameters of node to node anchor are summarized in Table 3. As the plate element is assumed to be fully connected to each other in the model, waler is thus not simulated in this research.

According to Ang et al. (2017), only two layers of soils and rocks are categorized of Case Waler, which is karst bedrock (limestone) underlying by loose sand. For simulating the behavior of soil and bedrock, two constitutive soil models were selected, HS model for the upper loose sand with drained and MC model for the limestone with undrained A. Advanced model is not eligible to be adopted due to limit of available and reliable site investigation data. The modeled soil profile is based on available borehole logs and site survey information. Due to limited results of in-situ tests and the condition of soil during the time of testing and sampling quality may be highly disturbed and the result by using empirical method to calibration by experience from previous study on similar ground condition. Table 4 summarizes the soil parameters of Case Waler. HS model is used for upper alluvium soil, Mohr-Coulomb (MC) model is used for rock simulation. The secant Young's modulus of soil is also taken with STP-N as below:

$$E_{50}^{ref} = 3000N \quad (4)$$

For this study, 6 of STP-N is selected.

Table 2 Diaphragm wall elastic properties (Plate element)

| Parameter | Name | Value | Unit |
|---|---|---|---|
| Compressive strength of concrete | fc' | 40 | MPa |
| Thickness | d | 0.6 | M |
| Young's modulus | E | 28 x $10^6$ | kPa |
| Young's modulus x 70% | 70% E | 19.6 x $10^6$ | kPa |
| Unit weight | w | 9 | kN/m$^3$ |
| Poisson's ratio | v | 0.2 | |

Table 3 Steel struts properties (Anchor element)

| Level | Strut size | Section Area (m$^2$) | EA (kN) | 60%EA (kN) |
|---|---|---|---|---|
| Level 1 | H400 x 400 | 0.0219 | 4.483 x $10^6$ | 2.6898 x $10^6$ |

Table 4 Input soil parameters of case CO

(a) Sandy soil

| Layer | Depth (m) | Drainage type | Unit weight (kN/m$^3$) | $c'_{ref}$ (kPa) | ϕ' (°) | $E_{50}^{ref}$ (kPa) |
|---|---|---|---|---|---|---|
| 1 | 0.0-25 | Drained | 19 | 1 | 29 | 18 x $10^3$ |

(b) Limestone (Mohr- Coulomb model)

| Layer | Depth (m) | Soil type | γ (kN/m$^3$) | $c'$ (kPa) | ϕ' (°) | $E'$ (kPa) |
|---|---|---|---|---|---|---|
| 2 | 25-104.5 | Limestone | 24 | 400 | 32 | 1 x $10^6$ |

Three types of plate element are adopted in this study and the input parameters of plate are summarized in Table 5. There are primary piles (a), secondary piles (b) and average piles (c). Equation (x) for secondary piles and average piles, equation (x) for primary wall caused of no steel rebar in the pile. Corresponding to the British Standard Institute (BS 8110), Young's modulus of concrete can be obtained by:

$$E = 20 + 0.2 \, x \, fc' \text{ (MPa)} \quad (5)$$

70% of Young's modulus is used for input parameters. The primary piles and secondary piles are modeled at the 17m spacing of struts.

Universal beam (UB) and universal column (UC) are selected for strutting system in Case CO, the steel grade of S 355 for UB and UC. Struts are also simulated by node to node anchor. Table 6 is the input parameters required by anchor element (strut).

Table 5 Various retaining wall properties

(a) Primary piles

| Parameter | Name | Value | Unit |
|---|---|---|---|
| Compressive strength of concrete | fc' | 40 | MPa |
| Thickness | d | 0.88 | M |
| Young's modulus | E | 28 x $10^6$ | kPa |
| Young's modulus x 70% | 70% E | 19.6 x $10^6$ | kPa |
| Unit weight | w | 9 | kN/m$^3$ |
| Poisson's ratio | v | 0.2 | - |

(b) Secondary piles

| Parameter | Name | Value | Unit |
|---|---|---|---|
| Compressive strength of concrete | fc' | 40 | MPa |
| Thickness | d | 1.48 | M |
| Young's modulus | E | $28 \times 10^6$ | kPa |
| Young's modulus x 70% | 70% E | $19.6 \times 10^6$ | kPa |
| Unit weight | w | 9 | kN/m$^3$ |
| Poisson's ratio | v | 0.2 | - |

(c) Average piles

| Parameter | Name | Value | Unit |
|---|---|---|---|
| Compressive strength of concrete | fc' | 40 | MPa |
| Thickness | d | 1.072 | M |
| Young's modulus | E | $28 \times 10^6$ | kPa |
| Young's modulus x 70% | 70% E | $19.6 \times 10^6$ | kPa |
| Unit weight | w | 9 | kN/m$^3$ |
| Poisson's ratio | v | 0.2 | - |

Table 6 Steel strut properties

| Level | Strut size | Section Area (m$^2$) | EA x $10^6$ (kN) | 60%EA x $10^6$ (kN) |
|---|---|---|---|---|
| 1 | 2-UB 610x324 | 0.106 | 21.73 | 13.038 |
| 2 | 2-UB 610x324 | 0.106 | 21.73 | 13.038 |
| 3 | 3-UB 610x324 | 0.159 | 32.56 | 19.557 |
| 4 | 3-UB 610x324 | 0.159 | 32.56 | 19.557 |
| 5 | 3-UB 610x324 | 0.159 | 32.56 | 19.557 |
| 6 | 3-UB 610x324 | 0.159 | $32.56^6$ | 19.557 |
| 7 | 3-UB 610x324 | 0.159 | 32.56 | 19.557 |
| 8 | 2-UB 610x324 | 0.106 | 21.73 | 13.038 |
| 9 | 2-UB 610x324 | 0.106 | 21.73 | 13.038 |

### 3.2 Computational sequences

The construction method of Case KLCC is bottom-up construction. Since the site only has one-layer of steel strut to support the retaining wall, so the total of construction phases in PLAXIS 3D are 5 phases, the depth of first excavation stage is 0.5 meter below the first struts layer, the simulation of phases is described at Table 7.

Table 7 Construction phase for case KLCC

| Phase | Construction |
|---|---|
| 0 | Initial phase (stress regeneration) |
| 1 | Installation of diaphragm wall |
| 2 | 1st stage excavation to 4.5 mbgl, dewatering to 5.5mbgl |
| 3 | Installation of 1st layer of struts |
| 4 | Excavation to purpose depth (13.2mbgl), dewatering to 14.2 mbgl |

For the preloading of steel struts is already created in the structure section as a point load instead of the prestress function of PLAXIS 3D by using point element. In calculation analysis, the calculation type of K0 procedure for initial phase and plastic analysis for the rest of construction phases, the calculation of pore pressure in all the construction phases are used phreatic. The calculation types are described as below (PLAXIS):

1. K0: Direct generation of initial effective stresses, pore pressures and state parameters;
2. Plastic: Elastoplastic drained or undrained analysis. Consolidation is not considered
3. Phreatic: Direct generation of steady-state pore pressures from phreatic level and cluster-related conditions.

Similarly, bottom-up construction method is also adopted for the Case Waler. Number of total excavation stages is 11 and the purpose excavation depth is 31.5 mbgl. There are 9-layers strut for supporting the retaining wall. For strutting excavation, every depth of excavation stage is 1 m below strut level and the excavation without any supporting system when the excavation starts from top of bedrock.

The actual prestress of the struts applied is around 20% to 30% of design strut load. Point load is used to simulate prestress of the struts at both ends of struts. Table 9 is the construction phase description for Case Waler.

Table 4.9 Construction phases of case CO

| Phase | Construction |
|---|---|
| 0 | Initial phase (stress regeneration) |
| 1 | Installation of second bored piles wall |
| 2 | 1st stage excavation to 3.5 mbgl, dewatering to 3.5 mbgl |
| 3 | Installation of 1st layer of struts at 2.5 mgbl |
| 4 | 2nd stage excavation to 7 mbgl, dewatering to 7 mbgl |
| 5 | Installation of 2nd layer of struts at 6 mgbl |
| 6 | 3rd stage excavation to 9 mbgl, dewatering to 9 mbgl |
| 7 | Installation of 3rd layer of struts at 8 mgbl |
| 8 | 4th stage excavation to 11 mbgl, dewatering to 11 mbgl |
| 9 | Installation of 4th layer of struts at 10 mgbl |
| 10 | 5th stage excavation to 14 mbgl, dewatering to 14 mbgl |
| 11 | Installation of 5th layer of struts at 13 mgbl |
| 12 | 6th stage excavation to 16 mbgl, dewatering to 16 mbgl |
| 13 | Installation of 6th layer of struts at 15 mgbl |
| 14 | 7th stage excavation to 18 mbgl, dewatering to 18 mbgl |
| 15 | Installation of 7th layer of struts at 17 mgbl |
| 16 | 8th stage excavation to 21.5 mbgl, dewatering to 21.5 mbgl |
| 17 | Installation of 8th layer of struts at 20.5 mgbl |
| 18 | 9th stage excavation to 23.5 mbgl, dewatering to 23.5 mbgl |
| 19 | Installation of 9th layer of struts at 22.5 mgbl |
| 20 | 10th stage excavation to 25 mbgl (bedrock), dewatering to 25 mbgl |
| 21 | Excavation to purpose depth (31.5 mbgl), dewatering to 31.5 mbgl |

## 4 RESULTS AND DISCUSSIONS

From the Figure 9 is the comparison between the observation and numerical analysis of Case KLCC. The inclinometer name of IN-3 and IN-8 are installed at the approximately center of long walls and the lateral wall movement is no significant difference between inclinometers readings and result of numerical model analysis due to the cross-section might be in the plain strain condition. As illustrated in figure 9 (IN-1 and IN-10), modelling the wall underestimates the lateral wall movement possibly due to comparatively worse quality of vertical joint between the rectangular panel and L-shaped panel.

The location of IN-5 and IN-6 are stood along the complementary wall, the wall movement decreases while decreasing the distance from the corner. Although IN-5 is at the centre of complementary wall, but the wall movement at IN-5 is smaller than IN-3 and IN-8. The reason is IN-5 is located on a relatively short wall. Refer to the Figure 9, majority of inclinometers reading are in good agreement with the prediction expect the ones near the corner by reasons stated above.

For Case Waler, this is the Class B analysis which means to do the analysis at the same time during occurrence of the event. Currently, the construction progress of the site is going to second excavation stage where excavate to 7 mbgl. This study only shows the comparison of first excavation stage between inclinometer readings and numerical analysis (Figure 10). There is significant difference between the readings and result. The difference between numerical analysis and inclinometer readings around 10 mm, the reasons may be caused by the capping beam at the top of SBPW is not simulated in the model or underestimation of the stiffness of upper alluvium soil.

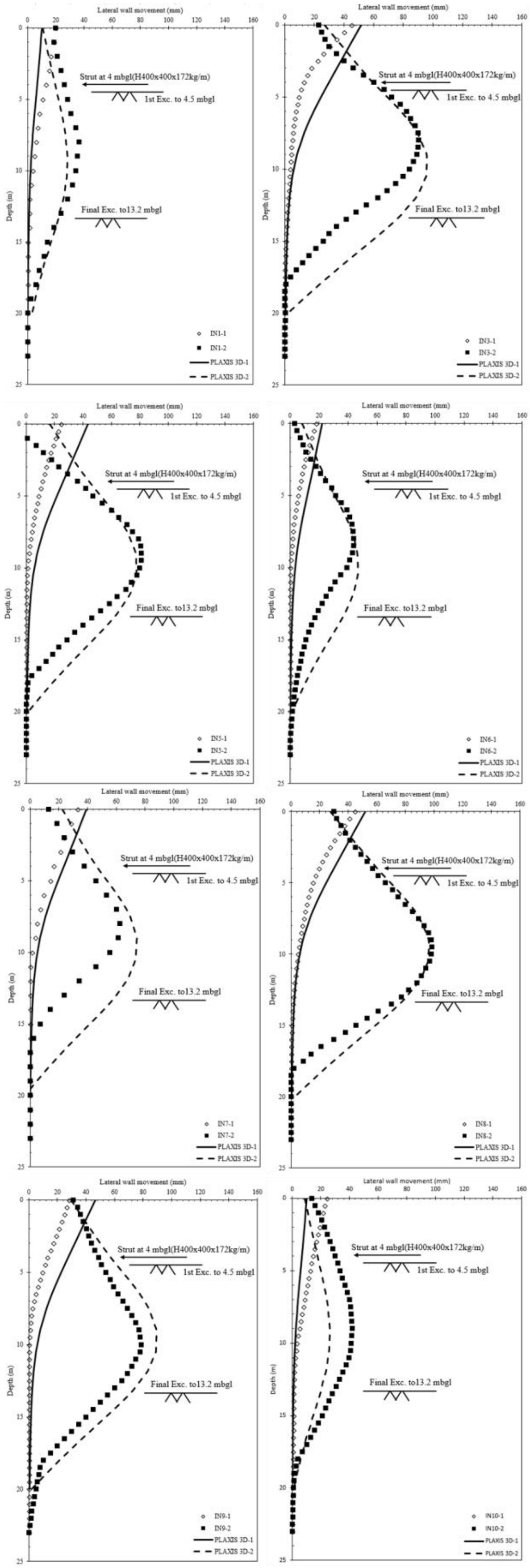


Figure 9 Comparison between observation and numerical analysis of Case KLCC

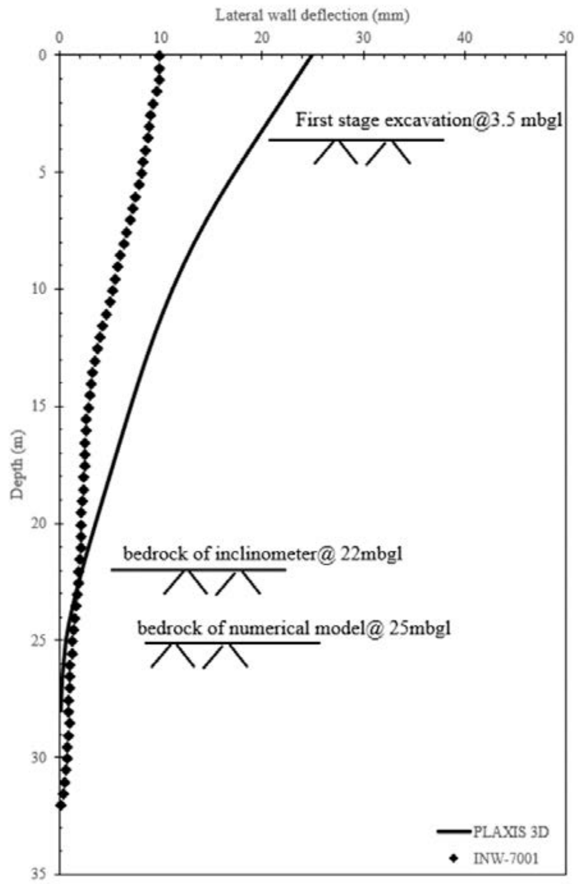


Figure 10 Comparison between observation and numerical analysis of Case Waler

The total displacement shading is shown as Figure 11 (a), shear force on wall indicated as Figure 11 (b) and bending moment on wall are illustrated as Figure 11 (c). Due to the axis of plate modelling is difference between PLAXIS in this study, the result of bending moment from PLAXIS is difference. From the result of PLAXIS, maximum shear force and bending moment of wall are 3069 kN/m and 4427 kNm/m respectively and both are located at the center of the 17 m spacing. The waler sizes which can take the shear force and bending moment is 2UC 400x400x283 kg/m, this waler size is selected for this condition. The shear capacity and bending moment capacity of 2UC 400x400x283 kg/m are 4520 kN and 5554kNm. The cross-section area of 2UC 400x400x283 kg/m is 0.0722 $m^2$.

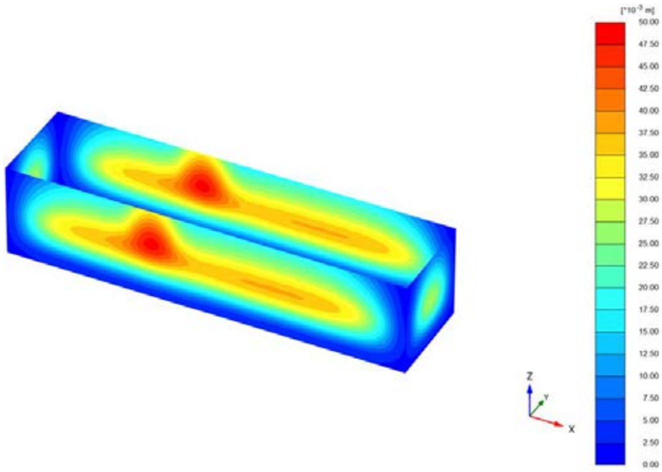

(a)

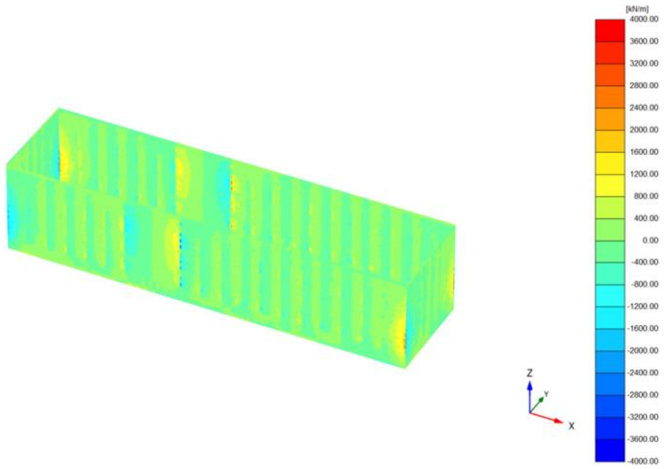

(b)

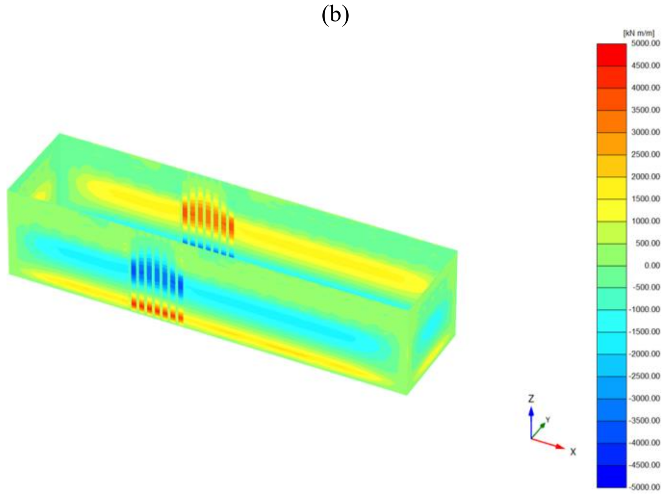

(c)

Figure 11 Result of numerical analysis: (a) total lateral wall displacement on wall; (b) shear force on wall; (c) bending moment on wall

To further evaluate the impacts from several factors which may influence PSR such as type of wall, horizontal spacing of waler, sizes of waler, parametric studies based on the same excavation model were conducted. By using the analytical results of case study of deep excavation in similar high permeability ground condition provided by Hsiung et al. (2016), named as Case A to compare with Case KLCC. The followings cases are simulated in this study:

1. Fully follow Case A:
   a. Horizontal and vertical strut spacing of Case A;
   b. Strut type of Case A;
   c. Retaining wall type of Case A;
2. Follow Case A strut and spacing, Case KLCC wall:
   a. Horizontal and vertical strut spacing of Case A;
   b. Strut type of Case A;
   c. Retaining wall type of Case KLCC;
3. Follow Case A strut spacing and wall, Case KLCC strut:
   a. Horizontal and vertical strut spacing of Case A;
   b. Strut type of Case KLCC;
   c. Retaining wall type of Case A;
4. Follow Case A strut and vertical spacing and wall, Case KLCC horizontal spacing:
   a. Vertical strut spacing of Case A;
   b. Horizontal strut spacing of Case KLCC;
   c. Strut type of Case A;
   d. Retaining wall type of Case A;
5. Follow Case A strut and vertical spacing, Case KLCC horizontal spacing and wall:
   a. Vertical strut spacing of Case A;
   b. Horizontal strut spacing of Case KLCC;
   c. Strut type of case A;
   d. Retaining wall type of case KLCC

As refer to Figure 12, the impacts on PSR from factors stated above are presented. Table 8 is the summarized of the difference in percentage with the factor used to analysis in this study. The baseline of the difference is Kaohsiung sand which provided by Hsiung et al. (2016). In the Table 5.2, name of KHH stand for Case A. From the summary of the result, higher value of difference when increasing the value of B/L due to the larger width stiffness for the corner is low. Meanwhile, when excavated in the narrow excavation, strut sizes and strut spacing is the key impact for the wall deformation; impact of horizontal spacing for the PSR is significant. Overall of the result, the most impact for PSR is ground condition and arrangement of strutting system.

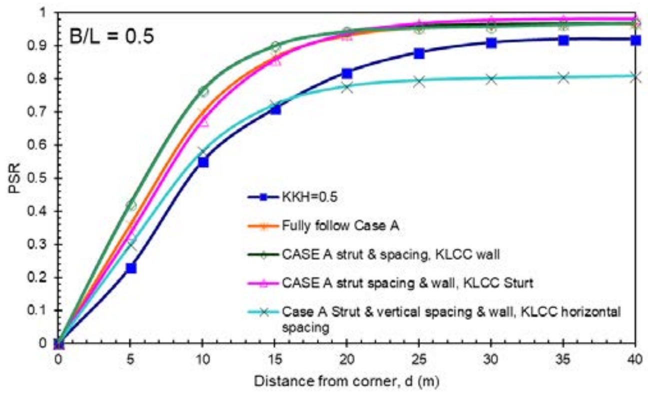


(a)

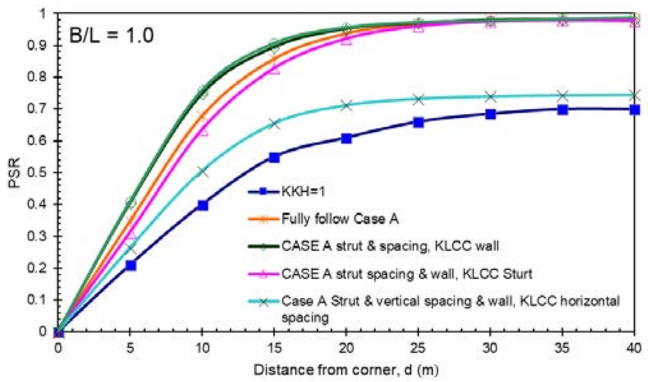


(b)

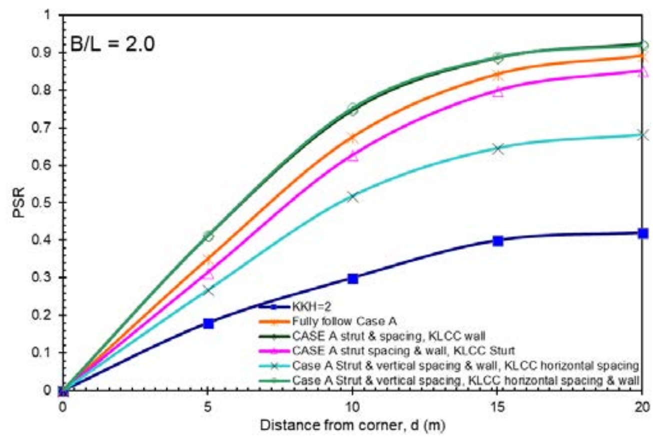


(c)

Figure 12 Variation of PSR with d for various value of ratio B and L: (a) B/L=0.5; (b) B/L=1; (c) B/L=2

Table 8 Summarized the difference of impact factors

(a) Difference of B/L =0.5 (B = 40 m, L = 80 m)

| **B/L = 0.5** | |
|---|---|
| Name of cases | Difference (%) |
| KKH | - |
| Fully follow case A | 5.178 |
| Case A strut & spacing & wall, KLCC wall | 5.39 |
| Case A strut & spacing & wall, KLCC strut | 6.82 |
| Case A strut &vertical spacing & wall, KLCC horizontal spacing | 12.16 |
| Case A strut & vertical spacing, KLCC horizontal spacing & wall | 5.35 |

(b) Difference of B/L =1 (B = 80 m, L = 80 m)

| **B/L = 1** | |
|---|---|
| Name of cases | Difference (%) |
| KKH | - |
| Fully follow case A | 40.28 |
| Case A strut & spacing & wall, KLCC wall | 39.81 |
| Case A strut & spacing & wall, KLCC strut | 39.68 |
| Case A strut &vertical spacing & wall, KLCC horizontal spacing | 6.5 |
| Case A strut & vertical spacing, KLCC horizontal spacing & wall | 41.088 |

(e) Difference of B/L =2 (B = 80 m, L = 40 m)

| **B/L = 2** | |
|---|---|
| Name of cases | Difference (%) |
| KKH | - |
| Fully follow case A | 112 |
| Case A strut & spacing & wall, KLCC wall | 120 |
| Case A strut & spacing & wall, KLCC strut | 103 |
| Case A strut &vertical spacing & wall, KLCC horizontal spacing | 62.28 |
| Case A strut & vertical spacing, KLCC horizontal spacing & wall | 119 |

For the evaluation of waler sizes, various depths of bedrock are given which are 7 mbgl, 11 mbgl, 14 mbgl, 18 mbgl, 21.5 mbgl and 25 mbgl. There is no additional support system when the excavation is beyond the bedrock level as the bedrock is recognized to be stiff enough to stabilize the ground. The depth of the lowest strut is only at above 1 m of the bedrock. The retaining wall is socketed 3 m into bedrock in every model and rock bolt is ignored in this study. Once the bedrock becomes shallower, the layer of strut where deeper than the bedrock will be removed.

From the numerical result of stresses on the wall, once the bedrock becomes shallower and retaining wall become shorter, the value of shear force and bending moment are lower, which mean the load from the wall to waler is lower, the sizes of waler can be smaller. Figure 13 is the relationship between stresses and depth of the retaining wall. The maximum shear force and bending moment on wall are located at the center of 17 m strut spacing.

Based on the numerical results and the calculation of the shear force and bending moment capacity of waler, the envelopes for the suitable sizes of waler for the strut spacing of 17 m has been established in this study and presented in Figure 14, the cross-section of the suitable strut size for x-axis of the chart, depth of bedrock for y-axis of the chart. Regarding the envelopes of Figure 14, the equation of the line regression is:

$$y = 288x + 4.8642 \quad (6)$$

where y is depth and cross-section area of waler is x in unit of $m^2$.

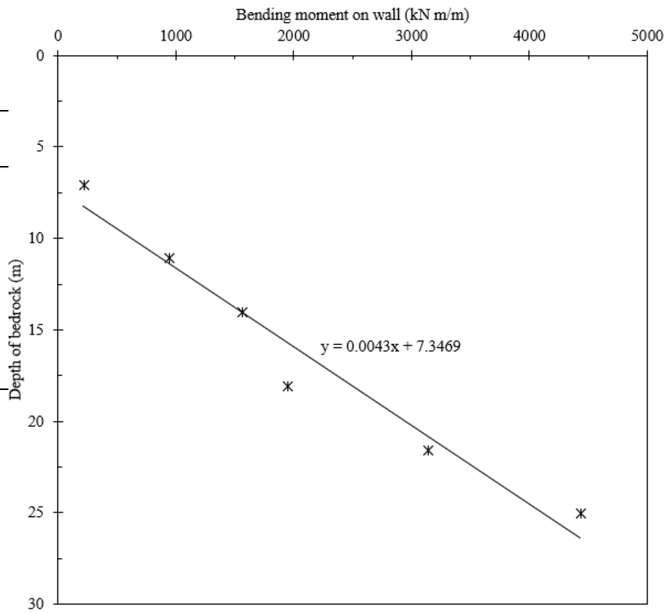


Figure 13 Relationship between maximum bending moment on wall and depth of bedrock

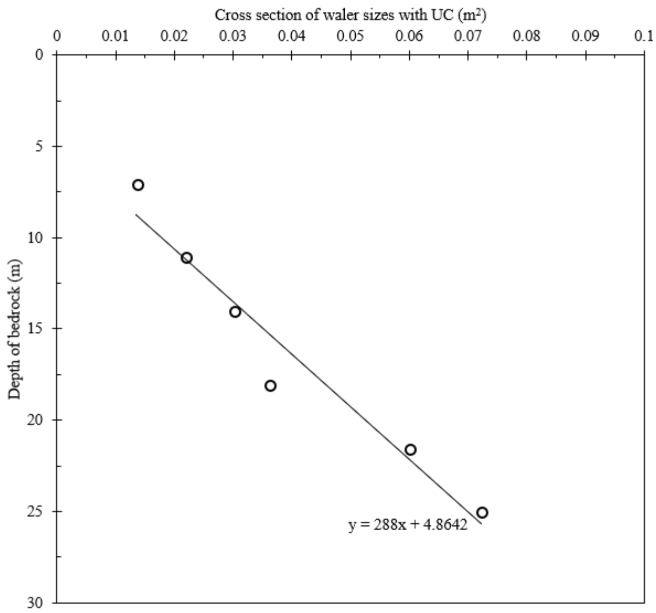


Figure 14 Envelope of suitable waler sizes for connect 17 m of spacing wall.

## 5 CONCLUSIONS

Based on this study, the following conclusions can be drawn by two parts:

For Case KLCC

1. It is aware that very limited information about site investigation and strut details are available so certain reasonable assumptions have to be made for analyses. Based on the result of the numerical analysis, majority of the observed field data clearly in good agreement with the prediction.
2. The wall where near the corner at the section of inclinometers (IN-1 and IN-10) are underestimated which might be due to comparatively worse quality of the vertical joint between the rectangular panel and L-shape panel of the wall and it thus induces a larger displacement from the observations.
3. Larger difference with increasing B/L is aware which is

due to the wider excavation has a low stiffness at the corner.

For Case Waler:

1. From the comparison between results of the numerical analysis and observations, it is likely the stiffness of soil is underestimated. As the result, the analysis might overestimate the lateral wall deflection.
2. Due to 3- dimensional characteristics of the model and software, the result of shear force and bending moment on wall from numerical analysis of PLAXIS3D is possible to be adopted for the evaluation of waler sizes.
3. The envelope of suitable waler size is suitable for prelim selection of the situation with 17 m of strut spacing in various depths of bedrock with upper alluvium soil.
4. The reason why having the 17 m of strut spacing is caused by the need to put a whole tunnel bored machine (TBM) from ground surface to purpose excavation level. The envelope of suitable waler size is a reference for selecting waler sizes in this kind of situation.

## 6 REFERENCES

Ang J. S., Hsiung B. C. B. and Wu, M. R. (2017) "Performance of Deep Excavation in Kuala Lumpur" Proceedings of the 17th Conference on Current Researches in Geotechnical Engineering in Taiwan.

Bishop, A. W. (1966) "The Strength of Soil as Engineering Materials" Geotechnique, pp91-128

Brinkgreve, R.B.J. et al., Editors (2012) "Plaxis 3D 2012 user's manual", Netherlands, Plaxis bv.

BS 5950: Part 1 (2000), Structure use of Steelwork in Building, Part 1: Code of Practice for Design and Construction, British Standards Institution

Chiew, S. P. and Leow, B. H. (2006) "Common Mistakes in Steel Design" International Symposium on Worldwide Trend and Development in Codified Design of Steel Structures. Kuala Lumpur, Malaysia.

Chogueur A., Abdeldjalil Z. and Reiffsteck P. (2018) "Parametric and Comparative Study of a Flexible Retaining wall" Periodica Polytechnica Civil Engineering, pp295-307

Eurocode 3 Part 1-1 (2005), Design of Steel Structures: Part 1-1 General Rules for Building, British Standards Institution

Ganno J. (2016) "Primary Firm Secant Pile Concrete Specification" Proceedings of the institution of Civil Engineers, pp110-120

H. Zabidi, M. Termizi, S. Aliman, K. S. Ariffin and N. L. Khalil (2015) "Geological Structure and Geomorphological Aspects in Karstified Susceptibility Mapping of Limestone Formations" 5th International Conference on Recent Advances in Materials, Minerals and Environment & 2nd International Postgraduate Conference on Materials, Mineral and Polymer, pp659-665

Hsiung, B. C. B. (2009) "A Case Study on the Behavior of a Deep Excavation in Sand. Comput. Geotechn. Pp.665-675

Hsiung, B. C. B., Hwang, R.N. (2009) "Evaluating Performance of Diaphragm walls by Wall Deflection Path. SEAGS. Special Issue on Excavation and Tunneling in Geotechnical Engineering, pp.81-90

Hsiung, B. C. B., Wang, C. L., Lin, H. T. and Chen C. H. (2013) "Design and Performance of a large-scale Excavation Adjacent to Sensitive Structures in Urban area" Proceedings of the 2nd International Conference on Geotechnics for Sustainable Development-Geotec. Hanoi, Vietnam

Hsiung, B. C. B., Yang, K. H., Aila, W., Hung, C., 2016. Three-dimensional Effects of a Deep Excavation on Wall Deflections in Loose to Medium Dense Sands. Comput. Geotechn.

Koo Kuan-Seng (2013), "Design and Construction of Excavation Works for Klang Valley Mass Rapid Transit Underground Station at Cochorance, Kuala Lumpur, Malaysia" Advances in Soil Mechanics and Geotechnical Engineering, Proceedings of the 5th International Young Geotechnical Engineers' Conference, pp559-563.

Law K. H., Ismail Z. and Roslan H. (2016) "3D Finite Element Analysis of a Deep Excavation Considering the Effect of Anisotropic Wall Stiffness" 19th Southeast Asian Geotechnical Conference & 2nd AGSSEA Conference (19SEAGC & 2AGSSEA) Kuala Lumpur, pp659-664.

Law K. H., Hashim, R. and Ismail Z. (2013) "Performance of Multipropped Deep Excavation in Kenny Hill Formation", Proc. 18th Southeast Asian Geotechnical Conference, Singapore, pp705-712.

Ou, C. Y., (2006) "Deep Excavation: Theory and Practice" Taylor & Francis, Netherlands

Ou, C. Y., Chiou, D.C., and Wu, T. S. (1996) "Three-dimensional Finite Element Analysis of Deep Excavations", Journal of Geotechnical and Geoenvironment Engineering, pp337-345

Schanz, T., Vermeer, P. A., and Bonnier, P. G. (1999) "The hardening soil model: formulation and verification", Beyond 2000 in Computational Geotechnics, Balkema, Rotterdam, pp281-296.

Skempton, A. W. (1986) "Standard Penetration Test Procedures" Geotechnique, vol. 36, no. 3, pp.425-557.

Tan, S. A. (2010) "One North Station Excavation in 30m of Jurong Residual Soils in Singapore", Earth Retention Conference, Washington, pp732-739.

Tan Siow Meng and Simon (2011) "Karstic Features of Kuala Lumpur Limestone"

Waltham, A. C. and Fookes, O.G. (2003) "Engineering classification of karst ground conditions". Quarterly Journal of Engineering Geology and Hydrogeology, pp101-118

Zdravkovic, L., Potts, D. M., and St Jogn, H. D. (2005) "Modelling of a 3D Excavation in Finite Element Analysis", Geotechnique, pp497-513.